

$\bar{B}_{d,s} \rightarrow K^{*0}\bar{K}^{*0}$ decays, a serious problem for the Standard Model

R. Aleksan¹, L. Oliver²

¹IRFU, CEA, Université Paris-Saclay, 91191 Gif-sur-Yvette cedex, France

²IJCLab, Pôle Théorie, CNRS/IN2P3 et Université Paris-Saclay,
Bât. 210, 91405 Orsay, France

May 16, 2024

ABSTRACT

We underline the theoretical and experimental interest of the vector-vector penguin decays $\bar{B}_{d,s} \rightarrow K^{*0}\bar{K}^{*0}$ for which the data show a strong U-spin violation. Indeed, with the latest LHCb data one has for these two modes very different longitudinal polarization fractions, $f_L^{exp}(\bar{B}_s \rightarrow K^{*0}\bar{K}^{*0}) = 0.24 \pm 0.04$ and $f_L^{exp}(\bar{B}_d \rightarrow K^{*0}\bar{K}^{*0}) = 0.74 \pm 0.05$. This feature is very striking because both modes are related by the exchange $s \leftrightarrow d$, i.e. they are related by U-spin symmetry as pointed out in earlier work by other authors. We illustrate this phenomenon by computing different observables for these modes within the QCD Factorization scheme, and we find, as expected, rather close values for the longitudinal fractions, with central values $f_L^{th}(\bar{B}_s \rightarrow K^{*0}\bar{K}^{*0}) \simeq 0.42$ and $f_L^{th}(\bar{B}_d \rightarrow K^{*0}\bar{K}^{*0}) \simeq 0.49$ and rather small errors. Furthermore, due to the $V - A$ nature of the weak currents and the heavy quark limit, one expects $(f_{\parallel}/f_{\perp})_{th} \simeq 1$, which in the B_s case is in contradiction with the data $(f_{\parallel}/f_{\perp})_{exp} \simeq 0.44 \pm 0.06$.

1 Introduction

In the absence of clear indications of physics beyond the Standard Model (SM), one may study in detail the rare decays of particles to search for deviations from the SM predictions. In this regard, B-meson decays to two vector particles are a very rich source of observables, which can exhibit signs of New Physics (NP). It has been shown that the decay $\bar{B}_s \rightarrow \phi\phi$ is a good candidate in order to search for evidence of NP [1], in particular at FCC-ee [2, 3, 4] where high sensitivities can be obtained. This can be achieved by searching for CP violating effects in time-dependent studies while almost no effect is expected in the Standard Model. Similar studies can be carried out with the decays $\bar{B}_s \rightarrow K^{*0}\bar{K}^{*0}$, with which sensitivities to NP can be improved further. In the present paper, we study this latter decay together with the decay $\bar{B}_d \rightarrow K^{*0}\bar{K}^{*0}$, which is related to the former through U-spin symmetry, and we show that it behaves in a way which is theoretically unexpected using QCD Factorization, thus requiring particular attention.

2 $B \rightarrow V_1 V_2$ experimental data

We summarize in Table 1 the available data on B decays to 2 light vector particles as given by the Particle Data Group (PDG) [5].

B decay	Br($\times 10^{-6}$)	f_L	f_{\parallel}	f_{\perp}	$f_{\parallel} - f_{\perp}$	A_{CP}
\overline{B}_s modes						
$\overline{B}_s \rightarrow \phi \rho^0$	0.27 ± 0.08	—	—	—	—	—
$\overline{B}_s \rightarrow \phi \phi$	18.5 ± 1.4	0.378 ± 0.013	<i>0.330 ± 0.016</i>	0.292 ± 0.009	0.038 ± 0.022	—
$\overline{B}_s \rightarrow \overline{K}^{*0} K^{*0}$	11.1 ± 2.7	0.24 ± 0.04	$0.297 \pm 0.049^*$	$0.38 \pm 0.12^*$	$-0.08 \pm 0.13^*$	—
$\overline{B}_s \rightarrow \phi K^{*0}$	1.14 ± 0.30	0.51 ± 0.17	0.21 ± 0.11	<i>0.28 ± 0.20</i>	-0.07 ± 0.28	—
\overline{B}_d modes						
$\overline{B}^0 \rightarrow \omega \omega$	1.2 ± 0.4	—	—	—	—	—
$\overline{B}^0 \rightarrow \rho^+ \rho^-$	27.7 ± 1.9	$0.990 \pm_{0.019}^{0.021}$	—	—	—	—
$\overline{B}^0 \rightarrow \rho^0 \rho^0$	0.96 ± 0.15	$0.71 \pm_{0.09}^{0.08}$	—	—	—	—
$\overline{B}^0 \rightarrow \rho^+ K^{*-}$	10.3 ± 2.6	0.38 ± 0.13	—	—	—	0.21 ± 0.15
$\overline{B}^0 \rightarrow \rho^0 \overline{K}^{*0}$	3.9 ± 1.3	0.173 ± 0.026	<i>0.426 ± 0.048</i>	0.401 ± 0.040	0.025 ± 0.084	-0.16 ± 0.06
$\overline{B}^0 \rightarrow \omega \overline{K}^{*0}$	2.0 ± 0.5	0.69 ± 0.11	<i>0.21 ± 0.17</i>	0.10 ± 0.13	0.11 ± 0.28	0.45 ± 0.25
$\overline{B}^0 \rightarrow \overline{K}^{*0} \phi$	10.0 ± 0.5	0.497 ± 0.017	<i>0.279 ± 0.023</i>	0.224 ± 0.015	0.055 ± 0.034	0.00 ± 0.04
$\overline{B}^0 \rightarrow K^{*0} \overline{K}^{*0}$	0.83 ± 0.24	0.74 ± 0.05	—*	—*	—*	—
B_u modes						
$B^- \rightarrow \omega K^{*-}$	< 7.4	0.41 ± 0.18	—	—	—	0.29 ± 0.35
$B^- \rightarrow \omega \rho^-$	15.9 ± 2.1	0.90 ± 0.06	—	—	—	-0.20 ± 0.09
$B^- \rightarrow \rho^0 \rho^-$	24.0 ± 1.9	0.950 ± 0.016	—	—	—	-0.05 ± 0.05
$B^- \rightarrow \rho^0 K^{*-}$	4.6 ± 1.1	0.78 ± 0.12	—	—	—	0.31 ± 0.13
$B^- \rightarrow \rho^- \overline{K}^{*0}$	9.2 ± 1.5	0.48 ± 0.08	—	—	—	-0.01 ± 0.16
$B^- \rightarrow K^{*-} \phi$	10.0 ± 2	0.50 ± 0.05	<i>0.30 ± 0.07</i>	0.20 ± 0.05	0.10 ± 0.12	-0.01 ± 0.08
$B^- \rightarrow K^{*-} K^{*0}$	0.91 ± 0.29	$0.82 \pm_{0.21}^{0.15}$	—	—	—	—

Table 1: B-meson branching fractions, f_L , f_{\parallel} , f_{\perp} and A_{CP} for some selected $V_1 V_2$ modes from the PDG [5]. Statistical and systematic errors have been added in quadrature. The values in italic are not measured directly but are deduced from $f_L + f_{\parallel} + f_{\perp} = 1$. * For these modes, LHCb has made more precise measurements not included by PDG and quoted below in the text.

In this Table 1, the Branching fractions and polarizations fractions are CP averages, i.e.

$$\begin{aligned}
 \text{Br} &= \frac{1}{2}[\text{Br}(B_{d,s} \rightarrow f) + \text{Br}(\overline{B}_{d,s} \rightarrow \overline{f})] \\
 f_{L,\parallel,\perp} &= \frac{1}{2}[f_{L,\parallel,\perp}(B_{d,s} \rightarrow f) + f_{L,\parallel,\perp}(\overline{B}_{d,s} \rightarrow \overline{f})] \\
 A_{CP} &= \frac{\text{Br}(\overline{B}_{d,s} \rightarrow \overline{f}) - \text{Br}(B_{d,s} \rightarrow f)}{\text{Br}(\overline{B}_{d,s} \rightarrow \overline{f}) + \text{Br}(B_{d,s} \rightarrow f)} \\
 A_{CP}^h &= \frac{f_h(\overline{B}_{d,s} \rightarrow \overline{f}) - f_h(B_{d,s} \rightarrow f)}{f_h(\overline{B}_{d,s} \rightarrow \overline{f}) + f_h(B_{d,s} \rightarrow f)} \quad \text{with } h = L, \parallel, \perp
 \end{aligned} \tag{1}$$

It is important to note that LHCb has measured f_L , f_{\parallel} and f_{\perp} for $\overline{B}_s \rightarrow K^{*0} \overline{K}^{*0}$ [6] more precisely and finds

$$f_L = 0.240 \pm 0.040 \quad , \quad f_{\parallel} = 0.234 \pm 0.027 \quad , \quad f_{\perp} = 0.526 \pm 0.037 \tag{2}$$

leading to $\Delta_{f_{\parallel,\perp}} = f_{\parallel} - f_{\perp} = -0.292 \pm 0.046$, i.e. $\neq 0$ at 6.4σ . LHCb has also measured f_L , f_{\parallel} and f_{\perp} for $\bar{B}_d \rightarrow K^{*0} \bar{K}^{*0}$ [6] and finds

$$f_L = 0.724 \pm 0.053 \quad , \quad f_{\parallel} = 0.116 \pm 0.035 \quad , \quad f_{\perp} = 0.160 \pm 0.046 \quad (3)$$

We note that, for this mode, $f_{\parallel} - f_{\perp} = -0.044 \pm 0.058$, i.e. compatible with $\Delta_{f_{\parallel,\perp}} = 0$. In summary, using the LHCb data, one has two striking features, which will be discussed further :

$$\left(\frac{f_{\parallel}^{\bar{B}_s \rightarrow K^{*0} \bar{K}^{*0}}}{f_{\perp}^{\bar{B}_s \rightarrow K^{*0} \bar{K}^{*0}}} \right)_{\text{LHCb}} = 0.44 \pm 0.06 \quad (4)$$

$$\left(\frac{f_L^{\bar{B}_d \rightarrow K^{*0} \bar{K}^{*0}}}{f_L^{\bar{B}_s \rightarrow K^{*0} \bar{K}^{*0}}} \right)_{\text{LHCb}} = 3.02 \pm 0.55 \quad (5)$$

3 Expectations using Naive Factorization

A detailed theoretical study of $\bar{B} \rightarrow V_1 V_2$ has been carried out [7] using QCD Factorization. In the following, we summarize the theoretical expectations using the values of the parameters shown in the Tables 2, 3 and 4.

In $\bar{B} \rightarrow V_1 V_2$ decays, one is dealing with 3 helicity amplitudes.

$$\bar{\mathcal{A}}_0 = A[\bar{B} \rightarrow V_1(0)V_2(0)] \quad , \quad \bar{\mathcal{A}}_{\pm} = A[\bar{B} \rightarrow V_1(\pm)V_2(\pm)] \quad (6)$$

Moving from the helicity representation to the transversity one, one gets :

$$\begin{aligned} \bar{\mathcal{A}}_L &= \bar{\mathcal{A}}_0 \\ \bar{\mathcal{A}}_{\parallel} &= \frac{\bar{\mathcal{A}}_+ + \bar{\mathcal{A}}_-}{\sqrt{2}} \quad , \quad \bar{\mathcal{A}}_{\perp} = \frac{\bar{\mathcal{A}}_+ - \bar{\mathcal{A}}_-}{\sqrt{2}} \end{aligned} \quad (7)$$

with the corresponding transversity rate fractions f_L , f_{\parallel} and f_{\perp} satisfying

$$f_L + f_{\parallel} + f_{\perp} = 1 \quad (8)$$

From Beneke et al. [12], one has :

$$\begin{aligned} \bar{\mathcal{A}}_0^{V_1 V_2} &= i \frac{G_F}{\sqrt{2}} m_B^2 f_{V_2} A_0^{B \rightarrow V_1}(0) \\ \bar{\mathcal{A}}_{\pm}^{V_1 V_2} &= i \frac{G_F}{\sqrt{2}} m_B m_{V_2} f_{V_2} F_{\pm}^{B \rightarrow V_1}(0) \end{aligned} \quad (9)$$

with

$$F_{\pm}^{B \rightarrow V_1}(q^2) \equiv \left(1 + \frac{m_1}{m_B}\right) A_1^{B \rightarrow V_1}(q^2) \mp \left(1 - \frac{m_1}{m_B}\right) V^{B \rightarrow V_1}(q^2) \quad (10)$$

Since the final quark is dominantly left-handed because of the $V-A$ structure of the Standard Model, heavy quark symmetry implies the hierarchy

$$\bar{\mathcal{A}}_L : \bar{\mathcal{A}}_{\perp} : \bar{\mathcal{A}}_+ = 1 : \frac{\Lambda_{QCD}}{m_b} : \left(\frac{\Lambda_{QCD}}{m_b}\right)^2 \quad (11)$$

The transverse amplitude $\bar{\mathcal{A}}_-$ is suppressed by factor m_{V_2}/m_b relative to $\bar{\mathcal{A}}_L$, and the axial and vector contributions to $\bar{\mathcal{A}}_+$ cancel out in the heavy quark limit and large recoil energy for the light mesons. Indeed, in this latter limit, the A_1 and V form factors are related and one has [8]

$$\begin{aligned} \frac{m_B}{m_B+m_V}V(q^2) &= \frac{m_B+m_V}{2E}A_1(q^2) \\ \text{with } E &= (m_B^2 + m_V^2 - q^2)/2m_B \end{aligned} \quad (12)$$

At $q^2 = 0$, one gets $2Em_B = m_B^2 + m_V^2$ and therefore in the limit $m_V \ll m_B$,

$$\frac{V(0)}{A_1(0)} \simeq 1 \quad (13)$$

giving in the heavy quark limit and large recoil energy for the light meson,

$$\bar{\mathcal{A}}_+ \simeq 0 \quad (14)$$

and one then has

$$\begin{aligned} \bar{\mathcal{A}}_{\parallel} \simeq -\bar{\mathcal{A}}_{\perp} &\simeq \frac{\bar{\mathcal{A}}_-}{\sqrt{2}} \\ |\bar{\mathcal{A}}_{\parallel}|^2 + |\bar{\mathcal{A}}_{\perp}|^2 &\simeq |\bar{\mathcal{A}}_-|^2 \equiv |\bar{\mathcal{A}}_T|^2 \end{aligned} \quad (15)$$

With the hierarchy above and the limit $\bar{\mathcal{A}}_+ \simeq 0$, one gets

$$f_{\parallel} \simeq f_{\perp} \quad (16)$$

Accordingly, we are left with only one transverse form factor $F_T^{B_{d,s} \rightarrow x}(0) \equiv F_-^{B_{d,s} \rightarrow x}(0)$. As can be seen in Table 1, the experiment is in agreement with equations (15) within errors, with the noticeable exception of $\bar{B}_s \rightarrow K^{*0}\bar{K}^{*0}$ if one uses the LHCb measurements of formula (2). This latter mode is discussed further in this note.

In most Penguin dominated decays such as $\bar{B}_s \rightarrow \phi\phi$, as we have exposed in detail in [1], although the equality $f_{\parallel} \simeq f_{\perp}$ is approximately satisfied by the data, the longitudinal fraction f_L is experimentally much smaller, of the order of $f_{\parallel,\perp}$, a feature that is qualitatively described within the QCD Factorization (QCDF) scheme [9, 10, 11], in papers devoted to the B decays to two vector mesons $\bar{B}_{d,s} \rightarrow V_1V_2$ [12, 13, 14, 15].

4 $\bar{B}_{d,s} \rightarrow K^{*0}\bar{K}^{*0}$ decays using QCD Factorization

We will now focus on the decays $\bar{B}_{d,s} \rightarrow K^{*0}\bar{K}^{*0}$. The important point that we want to underline is that these two decays are related by U -spin symmetry $d \leftrightarrow s$, as shown in all generality in Fig. 1 and already pointed out in e.g. [6, 16, 17, 18, 19, 20]. Therefore, the observables $f_{L,\parallel,\perp}$ in both decays should be equal in the limit of exact $SU(3)$ symmetry.

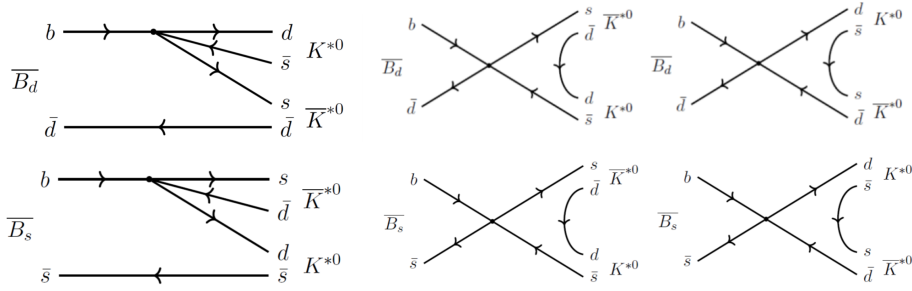


Figure 1: U -spin symmetry relates the modes $\bar{B}_s \rightarrow K^{*0}\bar{K}^{*0}$ and $\bar{B}_d \rightarrow K^{*0}\bar{K}^{*0}$.

However, the experimental results of LHCb [6] noted in (2) and (3) strongly contradicts this expectation.

In the limit of Naive Factorization, the amplitudes for the modes $\bar{B}_s \rightarrow K^{*0}\bar{K}^{*0}$ and $\bar{B}_d \rightarrow K^{*0}\bar{K}^{*0}$ are respectively governed by the products of CKM factors

$$\begin{aligned} A(\bar{B}_s \rightarrow K^{*0}\bar{K}^{*0}) &\sim \lambda'_t = V_{tb}V_{ts}^* = -\lambda'_u - \lambda'_c \\ A(\bar{B}_d \rightarrow K^{*0}\bar{K}^{*0}) &\sim \lambda_t = V_{tb}V_{td}^* = -\lambda_u - \lambda_c \end{aligned} \quad (17)$$

and the expected ratio of rates is of the order of magnitude

$$\frac{\text{Br}(\bar{B}_d \rightarrow K^{*0}\bar{K}^{*0})}{\text{Br}(\bar{B}_s \rightarrow K^{*0}\bar{K}^{*0})} \simeq 0.046 \quad (18)$$

i.e. consistent within errors with the branching ratios of Table 1,

$$\left[\frac{\text{Br}(\bar{B}_d \rightarrow K^{*0}\bar{K}^{*0})}{\text{Br}(\bar{B}_s \rightarrow K^{*0}\bar{K}^{*0})} \right]_{\text{exp}} = 0.075 \pm 0.028 \quad (19)$$

We conclude that, for the time being, it does not seem to be a contradiction between theory and experiment for the rates.

Of course, the hadronic parameters like form factors and decay constants are not the same for both modes. This feature will introduce some U -spin violation. To have a reasonable estimation of this U -spin violation, we will now compute the observables for both decays within QCD Factorization.

Following the notation of [1], the amplitudes of both modes write

$$\begin{aligned} A(\bar{B}_s \rightarrow K^{*0}\bar{K}^{*0}, h) &= \sum_{p=u,c} \lambda'_p S^{p,h} A^h(\bar{B}_s \rightarrow K^{*0}\bar{K}^{*0}) \\ &+ (\lambda'_u + \lambda'_c) T^h B^h(\bar{B}_s \rightarrow K^{*0}\bar{K}^{*0}) \end{aligned} \quad (20)$$

$$\begin{aligned} A(\bar{B}_d \rightarrow K^{*0}\bar{K}^{*0}, h) &= \sum_{p=u,c} \lambda_p S^{p,h} A^h(\bar{B}_d \rightarrow K^{*0}\bar{K}^{*0}) \\ &+ (\lambda_u + \lambda_c) T^h B^h(\bar{B}_d \rightarrow K^{*0}\bar{K}^{*0}) \end{aligned} \quad (21)$$

where the first terms describe the production-emission decays and the second ones correspond to the annihilation, as described in Fig. 1 and the CKM factors are given in Table 2,

λ_u	$V_{ub}V_{ud}^*$	$(0.001286 \pm 0.000152) - (0.003268 \pm 0.000115)i$
λ_c	$V_{cb}V_{cd}^*$	$(-0.009174 \pm 0.000161) + (5.370 \pm 0.267) \cdot 10^{-6}i$
λ'_u	$V_{ub}V_{us}^*$	$(0.000299 \pm 0.000035) - (0.000760 \pm 0.000027)i$
λ'_c	$V_{cb}V_{cs}^*$	$(0.03944 \pm 0.00069) + (1.249 \pm 0.006) \cdot 10^{-6}i$

Table 2: CKM parameters.

The coefficients A^h and B^h in (20,21) read for both modes and $h = 0, -$

$$A^0(\bar{B}_s \rightarrow K^{*0}\bar{K}^{*0}) = i\frac{G_F}{\sqrt{2}} m_{B_s}^2 A_0^{\bar{B}_s \rightarrow \bar{K}^{*0}} (m_{K^{*0}}^2) f_{K^{*0}} \quad (22)$$

$$A^-(\bar{B}_s \rightarrow K^{*0}\bar{K}^{*0}) = i\frac{G_F}{\sqrt{2}} m_{B_s} m_{K^{*0}} F_-^{\bar{B}_s \rightarrow \bar{K}^{*0}} (m_{K^{*0}}^2) f_{K^{*0}} \quad (23)$$

$$B^0(\bar{B}_s \rightarrow K^{*0}\bar{K}^{*0}) = B^-(\bar{B}_s \rightarrow K^{*0}\bar{K}^{*0}) = i\frac{G_F}{\sqrt{2}} f_{B_s} f_{K^{*0}}^2 \quad (24)$$

$$A^0(\bar{B}_d \rightarrow K^{*0}\bar{K}^{*0}) = i\frac{G_F}{\sqrt{2}} m_{B_d}^2 A_0^{\bar{B}_d \rightarrow \bar{K}^{*0}} (m_{K^{*0}}^2) f_{K^{*0}} \quad (25)$$

$$A^-(\bar{B}_d \rightarrow K^{*0}\bar{K}^{*0}) = i\frac{G_F}{\sqrt{2}} m_{B_d} m_{K^{*0}} F_-^{\bar{B}_d \rightarrow \bar{K}^{*0}} (m_{K^{*0}}^2) f_{K^{*0}} \quad (26)$$

$$B^0(\bar{B}_d \rightarrow K^{*0}\bar{K}^{*0}) = B^-(\bar{B}_d \rightarrow K^{*0}\bar{K}^{*0}) = i\frac{G_F}{\sqrt{2}} f_{B_d} f_{K^{*0}}^2 \quad (27)$$

where the relevant form factors and decay constants with their uncertainties are given in Table 3 and Table 4.

particle x	$m_x (MeV)$	$f_x (MeV)$	$\tau_x (s)$
\bar{B}_u	5279.34 ± 0	$190. \pm 5$	$1.638 \cdot 10^{-12} \pm 0$
\bar{B}_d	5279.65 ± 0	$190. \pm 5$	$1.519 \cdot 10^{-12} \pm 0$
\bar{B}_s	5366.88 ± 0	$230. \pm 5$	$1.515 \cdot 10^{-12} \pm 0$

Table 3: B meson parameters.

In the particular case of $\bar{B}_{d,s} \rightarrow K^{*0}\bar{K}^{*0}$, the rest of the relevant quantities in terms of the QCDF coefficients are given by the expressions [15]

$$S^{p,h} = a_4^{p,h} - \frac{1}{2} a_{10}^{p,h} \quad (28)$$

$$T^h = b_3^h + 2b_4^h - \frac{1}{2} b_3^{h,EW} - b_4^{h,EW} \quad (29)$$

particle x	m_x (MeV)	f_x (MeV)	$A_0^{B_d \rightarrow x}$	$F_-^{B_d \rightarrow x}$	$A_0^{B_s \rightarrow x}$	$F_-^{B_s \rightarrow x}$
ρ^0	$775. \pm 0$	209 ± 5	0.30 ± 0.05	0.55 ± 0.06	n/a	n/a
ω	$782. \pm 0$	187 ± 5	0.25 ± 0.05	0.50 ± 0.06	n/a	n/a
K^{*0}	$895. \pm 0$	218 ± 5	0.39 ± 0.05	0.68 ± 0.06	0.33 ± 0.05	0.53 ± 0.06
ϕ	1019.5 ± 0	221 ± 5	n/a	n/a	0.38 ± 0.05	0.65 ± 0.06

Table 4: Light meson parameters and heavy to light form factors.

The coefficients a_i^0, b_i^0 for the helicity $h = 0$ are given in Tables 5 and 7, and a_i^-, b_i^- for the transverse helicity $h = -$ in Tables 6 and 7. The main source of uncertainty is due to these QCDF coefficients, as made explicit in these Tables 5-7.

We assume that the amplitude for the transverse helicity $h = +$ is negligible, according to the hierarchy (14,16).

Coefficient	$\text{Re}(a_i^0)$	$\text{Im}(a_i^0)$	$\sigma_g(a_i^0)$
a_1^0	$0.945 \pm 1\%$	$0.014 \pm 0\%$	$\pm 10\%$
a_2^0	$0.302 \pm 25\%$	$-0.081 \pm 0\%$	$\pm 10\%$
a_3^0	$-0.008 \pm 50\%$	$0.003 \pm 0\%$	$\pm 10\%$
a_4^{0u}	$-0.021 \pm 7\%$	$-0.014 \pm 0\%$	$\pm 10\%$
a_4^{0c}	$-0.029 \pm 5\%$	$-0.009 \pm 0\%$	$\pm 10\%$
a_5^0	$0.015 \pm 33\%$	$-0.003 \pm 0\%$	$\pm 10\%$
a_7^{0u}/α	$-0.271 \pm 110\%$	$-0.680 \pm 98\%$	$\pm 10\%$
a_7^{0c}/α	$0.020 \pm 20\%$	$0.004 \pm 0\%$	$\pm 10\%$
a_9^{0u}/α	$-1.365 \pm 22\%$	$-0.680 \pm 95\%$	$\pm 10\%$
a_9^{0c}/α	$-1.058 \pm 2\%$	$-0.018 \pm 0\%$	$\pm 10\%$
a_{10}^{0u}/α	$-0.334 \pm 25\%$	$0.080 \pm 0\%$	$\pm 10\%$
a_{10}^{0c}/α	$-0.340 \pm 23\%$	$0.083 \pm 0\%$	$\pm 10\%$

Table 5: The a_i^0 QCDF coefficients for the helicity $h = 0$. $\sigma_g(a_i^0)$ is an additional error added in quadrature with the specific errors of a_i^0 .

In the present paper we only make explicit the calculations and results for the decay modes $\bar{B}_{d,s} \rightarrow K^{*0} \bar{K}^{*0}$. The rest of the decay modes for which there are presently experimental data, made explicit in Table 1 above, will be studied in detail in a forthcoming paper [7], and we only quote here the final results. Gathering all the parameters we find the expected values of the different observables, BR, f_L and A_{CP} obtained within QCD Factorization, as made explicit in Table 8. The various contributing errors for each parameter are assumed to be a flat distribution in the uncertainty range given in the Tables 2 to 7.

From the values for the form factors, decay constants and QCDF coefficients of the Tables 2-7, one finds the values of the branching ratios (see Figure 2)

$$\begin{aligned}
\text{Br}(\bar{B}_d \rightarrow K^{*0} \bar{K}^{*0}) &= (0.40_{-0.05}^{+0.14}) \times 10^{-6} \\
\text{Br}(\bar{B}_s \rightarrow K^{*0} \bar{K}^{*0}) &= (7.68_{-0.10}^{+0.38}) \times 10^{-6}
\end{aligned}
\tag{30}$$

Coefficient	Re(a_i^-)	Im(a_i^-)	$\sigma_g(a_i^-)$
a_1^-	$1.126 \pm 1\%$	$0.029 \pm 0\%$	$\pm 10\%$
a_2^-	$-0.207 \pm 9\%$	$-0.162 \pm 0\%$	$\pm 10\%$
a_3^-	$0.021 \pm 16\%$	$0.005 \pm 0\%$	$\pm 10\%$
a_4^{-u}	$-0.045 \pm 1\%$	$-0.015 \pm 0\%$	$\pm 10\%$
a_4^{-c}	$-0.043 \pm 1\%$	$-0.001 \pm 0\%$	$\pm 10\%$
a_5^-	$-0.026 \pm 15\%$	$-0.006 \pm 0\%$	$\pm 10\%$
a_7^{-u}/α	$1.052 \pm 25\%$	$0.009 \pm 0\%$	$\pm 10\%$
a_7^{-c}/α	$1.024 \pm 25\%$	$0.009 \pm 0\%$	$\pm 10\%$
a_9^{-u}/α	$-0.279 \pm 99\%$	$-0.037 \pm 0\%$	$\pm 10\%$
a_9^{-c}/α	$-0.307 \pm 90\%$	$-0.037 \pm 0\%$	$\pm 10\%$
a_{10}^{-u}/α	$0.292 \pm 21\%$	$0.171 \pm 0\%$	$\pm 10\%$
a_{10}^{-c}/α	$0.293 \pm 21\%$	$0.182 \pm 0\%$	$\pm 10\%$

Table 6: The a_i^- QCDF coefficients for the transverse helicity $h = -$. $\sigma_g(a_i^-)$ is an additional error added in quadrature with the specific errors of a_i^- .

index i	Re(b_i^0)	Im(b_i^0)	Re(b_i^-)	Im(b_i^-)
1	9.692 ± 1.110	-4.052 ± 1.060	0.691 ± 0.040	0 ± 0
2	-3.038 ± 0.347	1.268 ± 0.331	-0.0217 ± 0.013	0 ± 0
3	3.372 ± 0.915	-3.784 ± 1.210	-3.736 ± 0.929	3.855 ± 1.210
4	-1.203 ± 0.138	0.503 ± 0.131	-0.086 ± 0.005	0 ± 0
3_{EW}	-0.123 ± 0.012	0.080 ± 0.023	0.0305 ± 0.0094	-0.0399 ± 0.0126
4_{EW}	0.035 ± 0.004	-0.015 ± 0.004	0.0025 ± 0.0001	0 ± 0

Table 7: The b_i^0 and b_i^- QCDF annihilation coefficients for the helicity $h = 0$ and $h = -$.

that give the ratio (see Figure 3)

$$\left[\frac{\text{Br}(\bar{\text{B}}_d \rightarrow \text{K}^{*0} \bar{\text{K}}^{*0})}{\text{Br}(\bar{\text{B}}_s \rightarrow \text{K}^{*0} \bar{\text{K}}^{*0})} \right]_{\text{QCDF}} = 0.044_{-0.003}^{+0.008} \quad (31)$$

that is very close to the naive value (18), i.e. with no evidence of U -spin breaking.

For the longitudinal fractions one finds, on the other hand, the central values (see Figure 4)

$$\begin{aligned} f_L(\bar{\text{B}}_d \rightarrow \text{K}^{*0} \bar{\text{K}}^{*0}) &= 0.50_{-0.08}^{+0.08} \\ f_L(\bar{\text{B}}_s \rightarrow \text{K}^{*0} \bar{\text{K}}^{*0}) &= 0.42_{-0.08}^{+0.09} \end{aligned} \quad (32)$$

that give the ratio (see Figure 3)

$$\left[\frac{f_L(\bar{\text{B}}_d \rightarrow \text{K}^{*0} \bar{\text{K}}^{*0})}{f_L(\bar{\text{B}}_s \rightarrow \text{K}^{*0} \bar{\text{K}}^{*0})} \right]_{\text{QCDF}} = 1.07_{-0.08}^{+0.19} \quad (33)$$

with some small evidence of a theoretical U -spin breaking.

The values (32) are nevertheless close to each other and are at serious odds with experiment (2) and (3) for f_L , and neither of these values agrees with

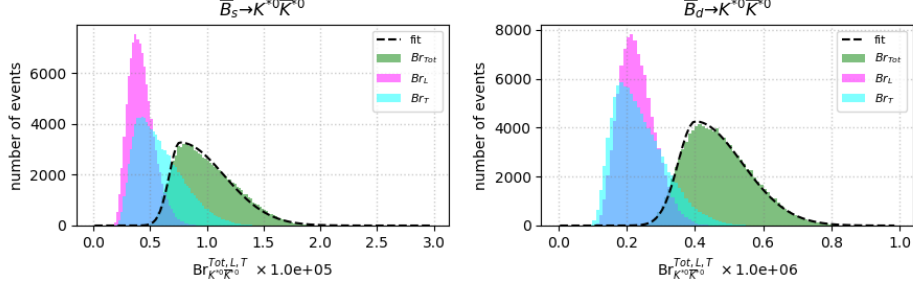


Figure 2: The CP-averaged Branching Fractions for a selection of $\bar{B}_{d,s}$ decays to $K^{*0}\bar{K}^{*0}$ final states. The written values correspond to QCD Factorization.

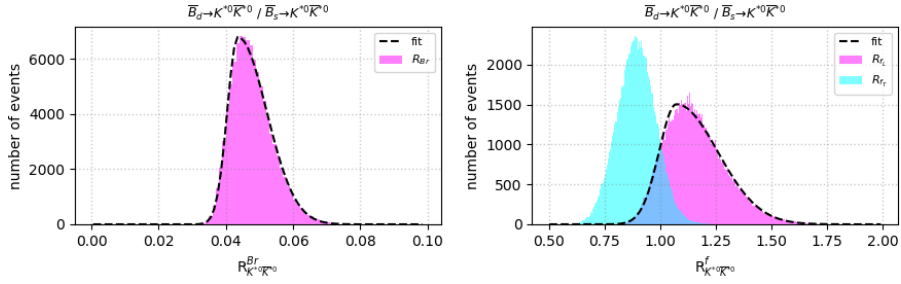


Figure 3: The ratio $\text{Br}(\bar{B}_d \rightarrow K^{*0}\bar{K}^{*0})/\text{Br}(\bar{B}_s \rightarrow K^{*0}\bar{K}^{*0})$ and $f_L(\bar{B}_d \rightarrow K^{*0}\bar{K}^{*0})/f_L(\bar{B}_s \rightarrow K^{*0}\bar{K}^{*0})$ as calculated with QCD Factorization.

experiment. The quantitative comparison of LHCb data in equation (5) with QCDF leads to

$$\left[\frac{f_L(\bar{B}_d \rightarrow K^{*0}\bar{K}^{*0})}{f_L(\bar{B}_s \rightarrow K^{*0}\bar{K}^{*0})} \right]_{\text{LHCb}} - \left[\frac{f_L(\bar{B}_d \rightarrow K^{*0}\bar{K}^{*0})}{f_L(\bar{B}_s \rightarrow K^{*0}\bar{K}^{*0})} \right]_{\text{QCDF}} = 1.96^{+0.56}_{-0.60} \quad (34)$$

which is a 3.3 standard deviation (std) effect. Should the experimental error on $f_L(\bar{B}_d \rightarrow K^{*0}\bar{K}^{*0})/f_L(\bar{B}_s \rightarrow K^{*0}\bar{K}^{*0})$ be reduced by a factor 2, the significance would exceed 5 std. Furthermore the expectation $f_{\parallel} \simeq f_{\perp}$ is strongly contradicted by the experimental LHCb data quoted in (2).

To compare the QCD Factorization predictions to the data, one should consider the Form Factor $F_+ \neq 0$, which will lead to $f_{\parallel} \neq f_{\perp}$. Equation (10) is used with values of A_1 and V estimated using light-cone sum rules [21]. As expected the central values $F_+^{B \rightarrow V} \simeq 0$ is obtained, though with some uncertainties. We follow the estimates from [12] and use the values in Table 9.

We summarize in Figure 5 the prediction from QCD Factorization, using the values of F_+ as given in Table 9. We conclude that the expectation of QCD Factorization is not compatible with the data for the decay $\bar{B}_s \rightarrow K^{*0}\bar{K}^{*0}$ and it is marginally compatible for $\bar{B}_d \rightarrow K^{*0}\bar{K}^{*0}$.

B decay	Br($\times 10^{-6}$)	f_L	f_{\parallel}	f_{\perp}	A_{CP}
\overline{B}_s modes					
$\overline{B}_s \rightarrow \phi \rho^0$	0.306 ± 0.059	0.951 ± 0.023	0.025 ± 0.012	0.025 ± 0.012	0.318 ± 0.034
$\overline{B}_s \rightarrow \phi \phi$	22.630 ± 6.670	0.315 ± 0.070	0.343 ± 0.035	0.343 ± 0.035	0.007 ± 0.002
$\overline{B}_s \rightarrow \overline{K}^{*0} K^{*0}$	10.050 ± 2.640	0.429 ± 0.088	0.286 ± 0.044	0.286 ± 0.044	0.006 ± 0.001
$\overline{B}_s \rightarrow \phi K^{*0}$	0.504 ± 0.163	0.365 ± 0.074	0.318 ± 0.037	0.318 ± 0.037	-0.160 ± 0.037
\overline{B}_d modes					
$\overline{B}^0 \rightarrow \omega \omega$	0.840 ± 0.204	0.914 ± 0.024	0.043 ± 0.012	0.043 ± 0.012	-0.416 ± 0.071
$\overline{B}^0 \rightarrow \rho^+ \rho^-$	23.840 ± 4.910	0.904 ± 0.023	0.048 ± 0.012	0.048 ± 0.012	-0.071 ± 0.015
$\overline{B}^0 \rightarrow \rho^0 \rho^0$	0.734 ± 0.203	0.841 ± 0.061	0.080 ± 0.031	0.080 ± 0.031	0.572 ± 0.099
$\overline{B}^0 \rightarrow \rho^+ K^{*-}$	6.973 ± 2.000	0.405 ± 0.062	0.298 ± 0.031	0.298 ± 0.031	0.305 ± 0.065
$\overline{B}^0 \rightarrow \rho^0 \overline{K}^{*0}$	3.446 ± 1.110	0.324 ± 0.070	0.338 ± 0.035	0.338 ± 0.035	-0.189 ± 0.040
$\overline{B}^0 \rightarrow \omega \overline{K}^{*0}$	2.932 ± 0.951	0.387 ± 0.085	0.307 ± 0.043	0.307 ± 0.043	0.187 ± 0.047
$\overline{B}^0 \rightarrow \overline{K}^{*0} \phi$	9.285 ± 2.550	0.340 ± 0.071	0.330 ± 0.036	0.330 ± 0.036	0.009 ± 0.002
$\overline{B}^0 \rightarrow K^{*0} \overline{K}^{*0}$	0.465 ± 0.095	0.498 ± 0.086	0.251 ± 0.043	0.251 ± 0.043	-0.165 ± 0.022
B_u modes					
$B^- \rightarrow \omega K^{*-}$	3.425 ± 0.990	0.419 ± 0.076	0.291 ± 0.038	0.291 ± 0.038	0.408 ± 0.087
$B^- \rightarrow \omega \rho^-$	13.140 ± 2.720	0.924 ± 0.022	0.038 ± 0.011	0.038 ± 0.011	-0.189 ± 0.037
$B^- \rightarrow \rho^0 \rho^-$	17.920 ± 3.910	0.956 ± 0.012	0.022 ± 0.006	0.022 ± 0.006	-0.000 ± 0.001
$B^- \rightarrow \rho^0 K^{*-}$	4.559 ± 1.000	0.535 ± 0.093	0.233 ± 0.0047	0.233 ± 0.0047	0.435 ± 0.054
$B^- \rightarrow \rho^- \overline{K}^{*0}$	7.242 ± 2.070	0.413 ± 0.082	0.294 ± 0.0041	0.294 ± 0.0041	-0.000 ± 0.001
$B^- \rightarrow K^{*-} \phi$	9.803 ± 2.630	0.337 ± 0.071	0.332 ± 0.036	0.332 ± 0.036	0.003 ± 0.034
$B^- \rightarrow K^{*-} K^{*0}$	0.443 ± 0.106	0.464 ± 0.081	0.268 ± 0.041	0.268 ± 0.041	-0.027 ± 0.034

Table 8: B-meson branching fractions, f_L , f_{\parallel} , f_{\perp} and A_{CP} for some selected V_1 - V_2 modes as calculated with QCD Factorization. The values in italics are derived from $f_{\parallel} = f_{\perp} = f_T/2 = (1 - f_L)/2$. This table is to be compared with the experimental Table 1.

5 Sensitivities at FCC-ee

We estimate now the sensitivities that can be attained at FCC-ee. To this end we have simulated a generic detector with parametrized resolutions described in detail in [22].

5.1 Detector simulation

In the following we summarize the main characteristics of the simulated detector. The components of this detector, which are relevant for this study, include a silicon pixelized vertex system, a large gaseous tracking device, an outer silicon wrapper and a ToF detector embedded in a solenoid with a field of 2 Tesla. The parametrizations of the vertex and tracking resolutions are

particle x	ρ	ω	K^*	ϕ
$F_+^{B_d \rightarrow x}$	$0. \pm 0.06$	$0. \pm 0.06$	$0. \pm 0.06$	n/a
$F_+^{B_s \rightarrow x}$	n/a	n/a	$0. \pm 0.06$	$0. \pm 0.06$

Table 9: F_+ form factors.

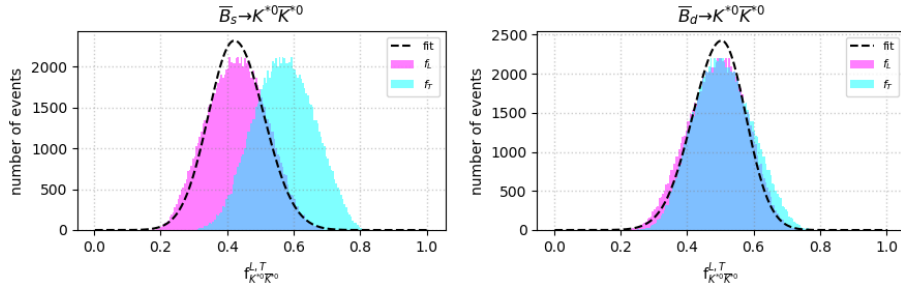


Figure 4: The CP-averaged fractions of longitudinal and transverse polarizations (f_L, f_T) for the decays of $\bar{B}_{d,s} \rightarrow K^{*0} \bar{K}^{*0}$ as calculated with QCD Factorization.

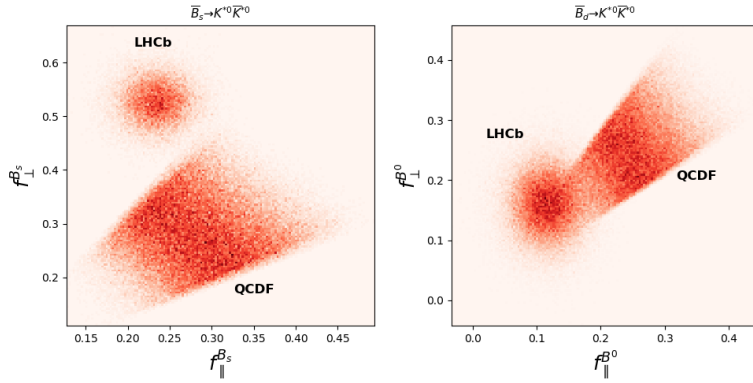


Figure 5: f_{\perp} versus f_{\parallel} as predicted by QCD Factorization using the form factors F_+ and F_- obtained from light-cone sum rules. The data from LHCb [6] are also displayed.

obtained by the simulation of the following components :

- *Silicon vertex and inner tracker* : The silicon detector includes 8 layers of pixel sensors with the main parameters listed in Table 10. It also includes 6 layers of disks in each end cap (Table 11).

layer	1	2	3	4	5	6	7	8
$r(cm)$	1.2	1.8	3.7	6.0	10.0	20.0	30.0	38.0
$z(\pm cm)$	20.0	23.0	20.0	60.0	60.0	60.0	60.0	64.0
X/X_0	0.001	0.001	0.001	0.001	0.001	0.001	0.007	0.007
$\sigma(\mu m)$	3.0	3.0	4.0	4.0	4.0	4.0	7.0	7.0

Table 10: Barrel silicon vertex and inner tracker parameters.

- *TPC* : The central tracking is achieved by a TPC, the main parameters of which are listed in Table 12.
- *Outer wrapper* : A silicon outer wrapper surrounding the TPC is included with a point resolution of $10\mu m$.

<i>layer</i>	1	2	3	4	5	6
innerR(<i>cm</i>)	5.5	5.5	11.5	11.5	16.5	16.5
outerR(<i>cm</i>)	38.5	38.5	38.5	38.5	38.5	38.5
<i>z</i> (<i>cm</i>)	65	80	150	170	220	240
<i>X/X</i> ₀	0.003	0.003	0.003	0.003	0.003	0.003
σ (μ <i>m</i>)	7.0	7.0	7.0	7.0	7.0	7.0

Table 11: End cap silicon vertex and inner tracker parameters.

innerR (<i>cm</i>)	outerR (<i>cm</i>)	<i>z</i> (<i>cm</i>)	Number layers	σ (<i>r</i>) μ <i>m</i>	σ (<i>z</i>) μ <i>m</i>
40	220	± 250	250	100	500

Table 12: The TPC tracker parameters.

The particle identification (PID) is achieved using a dedicated time-of-flight (*ToF*) system and the cluster counting (dN/dx) from the gaseous tracker with the resolutions $\sigma(\textit{ToF}) = 10ps$ and $\sigma(dN/dx) = 2.2\%$, respectively. With the tracking parameters above, some important resolutions are obtained for the decay $\bar{B}_{d,s} \rightarrow K^{*0}\bar{K}^{*0}$. It includes in particular the reconstructed error on B mass and on the B flight distance:

$$\begin{aligned}\sigma_{m_B} &\simeq 6 \textit{ MeV} \\ \sigma_{d_B} &\simeq 20 \mu\textit{m}\end{aligned}\tag{35}$$

These figures are instrumental to suppress the background very efficiently. Figure 6 shows the $(K^+\pi^-)(K^-\pi^+)$ mass for the channel $\bar{B}_s \rightarrow K^{*0}\bar{K}^{*0}$ and the K/ π separation. It should also be stressed that PID is very important for carrying out this study. Indeed, the combinatoric background from $Z \rightarrow q\bar{q}$ (mostly $Z \rightarrow b\bar{b}$) as well as final states such as $\bar{B} \rightarrow (K^+K^-)_\phi(K^-\pi^+)_{\bar{K}^{*0}}$ may lead to significant contribution if one has no or poor K/ π separation. Table 13 summarizes the expected number of produced $(K^+\pi^-)_{K^{*0}}(K^-\pi^+)_{\bar{K}^{*0}}$ final states from $B_{d,s}$ decays at the Z-pole at FCC.

Although small, the main source of background is expected to be of combinatorial origin. Inclusive Monte-Carlo samples of $Z \rightarrow b\bar{b}$ and $Z \rightarrow c\bar{c}$ events have been used to confirm this expectation, and to quantify the level of the combinatoric background. The generated samples consist of about 10^9 $b\bar{b}$ events and about $0.5 \cdot 10^9$ $c\bar{c}$ events produced with the PYTHIA 8.306 Monte-Carlo generator [23]. PYTHIA generates also signal events in this inclusive $b\bar{b}$ sample, however the branching fractions are different than the values of PDG. For $\bar{B}_d \rightarrow K^{*0}\bar{K}^{*0}$, PYTHIA uses 10^{-6} , instead of $0.83 \cdot 10^{-6}$ (PDG) and for $\bar{B}_s \rightarrow K^{*0}\bar{K}^{*0}$, PYTHIA uses $4 \cdot 10^{-6}$ instead of $11.1 \cdot 10^{-6}$ (PDG), i.e. a factor ~ 2.8 too low. This is not an issue since we are mainly interested in the evaluation of the background level. The generated events were passed through a fast simulation of the IDEA detector [4], which provides resolutions corresponding to a detector similar to the one described in this Section above. The simulation is based on DELPHES [24]. In particular, the simulation software that turns charged particles into simulated

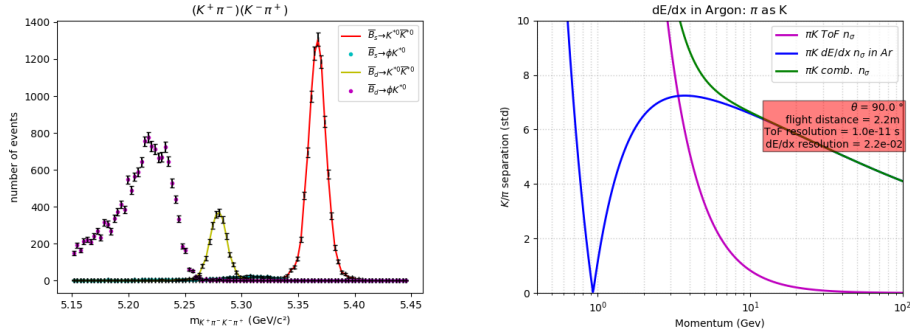


Figure 6: Invariant mass for $\bar{B}_{d,s} \rightarrow (K^+\pi^-)(K^-\pi^+)$ combinations without particle identification (left) and K/π separation expected with the simulated detector (right). The left plot shows also the contributions from $\bar{B}_d \rightarrow \phi\bar{K}^{*0}$ and $\bar{B}_s \rightarrow \phi K^{*0}$ where one of the K from ϕ is misidentify as a π . Combinatoric background is not shown neither possible contributions coming from $K_0^*(700)$, $K_0^*(1430)$..., which are however low.

tracks relies on a full description of the geometry of the IDEA vertex detector and drift chamber. The software accounts for the finite detector resolution and for the multiple scattering in each tracker layer and determines the (non diagonal) covariance matrix of the helix parameters that describe the trajectory of each charged particle. This matrix is then used to produce a smeared 5-parameters track, for each charged particle emitted within the angular acceptance of the tracker. Finally, the events were subsequently analysed within the FCCAnalyses framework [25].

The reconstruction of signal candidates starts with the identification of the “primary tracks”, that can be fit to a primary vertex¹, and, consequently, of the “secondary tracks”. Moreover, all reconstructed particles are used to determine the thrust axis, and the plane orthogonal to this axis and containing the interaction point divides each event in two hemispheres.

Quadruplets of secondary tracks with total charge 0 that belong to a same hemisphere are fit to a common vertex. A $\chi^2 < 20$ is requested. Furthermore, pairs of particles with invariant mass (determined from the tracks’ momenta at the fitted vertex) within $m_{K^{*0}} - 0.075$ and $m_{K^{*0}} + 0.075$ GeV define the K^{*0} and \bar{K}^{*0} candidates. The standalone vertex fit algorithm [26] used in this analysis is available in the distribution of the DELPHES package, and its recent extension to allow neutral particles to be included in the fit is described in [27]. Quadruplets with an invariant mass above 5.0 GeV and a momentum larger than 10 GeV are kept as potential B_s (B_d) candidates. Table 14 summarizes all cuts. We show in Figure 7 the B_d and B_s candidates without particle identification. A signal is observed both for B_d and B_s but significant background is present.

¹A simple iterative algorithm is used here. In a first step, all tracks are fit to a common vertex, using a constraint given by the beam-spot size. The track that gives the largest contribution to the χ^2 of the fit is removed, and the remaining tracks are fit again. The procedure is repeated until the χ^2 contribution of each track is below a given cut.

$E_{\text{cm}} = m_Z$ and $\int L = 150\text{ab}^{-1}$			
$\sigma(e^+e^- \rightarrow Z)$ nb	number of Z	$f(Z \rightarrow \bar{B}_s)$	Number of produced \bar{B}
~ 42.9	$\sim 6.4 \cdot 10^{12}$	0.0159	$\sim 1 \cdot 10^{11} \bar{B}_s$
~ 42.9	$\sim 6.4 \cdot 10^{12}$	0.0608	$\sim 3.9 \cdot 10^{11} \bar{B}_d$
\bar{B} decay Mode	K^{*0} Decay Mode	Final State	Number of \bar{B} decays
$\bar{B}_s \rightarrow K^{*0} \bar{K}^{*0}$	$K^+ \pi^-$	$K^+ \pi^- K^- \pi^+$	$\sim 4.9 \cdot 10^5$
$\bar{B}_d \rightarrow K^{*0} \bar{K}^{*0}$	$K^+ \pi^-$	$K^+ \pi^- K^- \pi^+$	$\sim 1.4 \cdot 10^5$

Table 13: The expected number of produced $\bar{B}_{d,s}$ decays to the specific decay mode $K^{*0} \bar{K}^{*0}$ at FCC-ee at a center of mass energy of m_Z over 4 years with 2 detectors. This number has to be multiplied by 2 when including $B_{d,s}$ decays. The branching fractions of the PDG [5] have been used.

<i>cuts</i>	tr.1 – 4	K^{*0} cand	\bar{K}^{*0} cand	$(K^{*0} \bar{K}^{*0})$ cand
$ \cos \theta $	< 0.95	n/a	n/a	n/a
p (GeV)	> 0.5	n/a	n/a	> 10.0
m (GeV)	PID	$m_{K^{*0}} \pm 0.075$	$m_{\bar{K}^{*0}} \pm 0.075$	$> 5.$
χ^2_{vtx}	n/a	n/a	n/a	20

Table 14: Summary of all cuts applied for selecting potential $B_{d,s}$ candidates. The overall selection efficiency is about 33%.

Turning on the particle identification the situation changes dramatically (see Figure 8). As it can be seen, despite the low Branching Fractions, the signal is clearly visible with essentially no combinatorial background. However, one notes that there is some peaking background. These events are due to non-resonant (n-r) backgrounds such as $B_{d,s} \rightarrow K^{*0} (K^- \pi^+)_{n-r}$, $B_{d,s} \rightarrow \bar{K}^{*0} (K^+ \pi^-)_{n-r}$ and at a lower level $B_{d,s} \rightarrow (K^\mp \pi^\pm K^\pm \pi^\mp)_{n-r}$.

5.2 A simple angular analysis

Finally, we have carried out a simple angular analysis, i.e. without background, which we have shown to be small should one have an excellent PID, as also demonstrated by LHCb [6]. To this end, we have generated $\bar{B}_{d,s}$ decays to $K^{*0} \bar{K}^{*0}$ with the polarization expected with our calculations using QCD factorization, shown in Table 8. In pseudoscalar decays to 2 vector resonances decaying in turn to 2 pseudoscalar particles, the full angular dependence of the cascade reads as [28]

$$\begin{aligned}
\frac{d\Gamma(\bar{B}_{d,s} \rightarrow K^{*0} \bar{K}^{*0})}{d\cos\theta_1 d\cos\theta_2 d\phi} &\propto |\bar{\mathcal{A}}_0|^2 \cos^2\theta_1 \cos^2\theta_2 + \frac{|\bar{\mathcal{A}}_+|^2 + |\bar{\mathcal{A}}_-|^2}{4} \sin^2\theta_1 \sin^2\theta_2 \\
&- [\Re(e^{-i\phi} \bar{\mathcal{A}}_0 \bar{\mathcal{A}}_+^*) + \Re(e^{i\phi} \bar{\mathcal{A}}_0 \bar{\mathcal{A}}_-^*)] \cos\theta_1 \sin\theta_1 \cos\theta_2 \sin\theta_2 \\
&+ \frac{\Re(e^{2i\phi} \bar{\mathcal{A}}_+ \bar{\mathcal{A}}_-^*)}{2} \sin^2\theta_1 \sin^2\theta_2
\end{aligned} \tag{36}$$

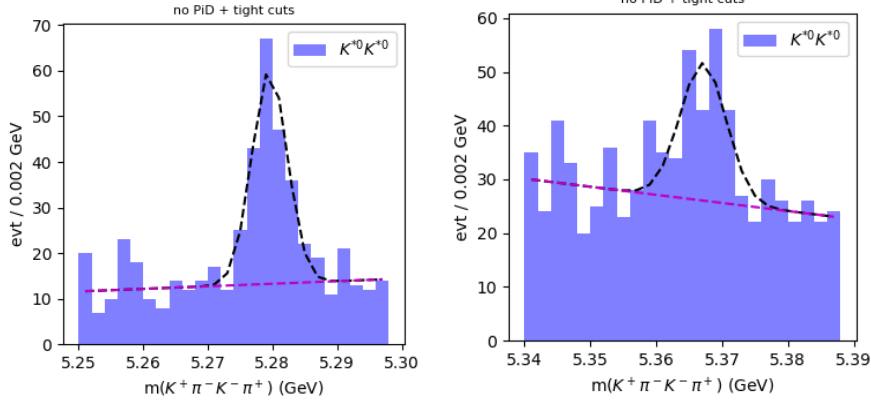


Figure 7: Invariant mass distribution for $\bar{B}_d \rightarrow K^{*0}\bar{K}^{*0}$ and $\bar{B}_s \rightarrow K^{*0}\bar{K}^{*0}$ candidates without particle identification.

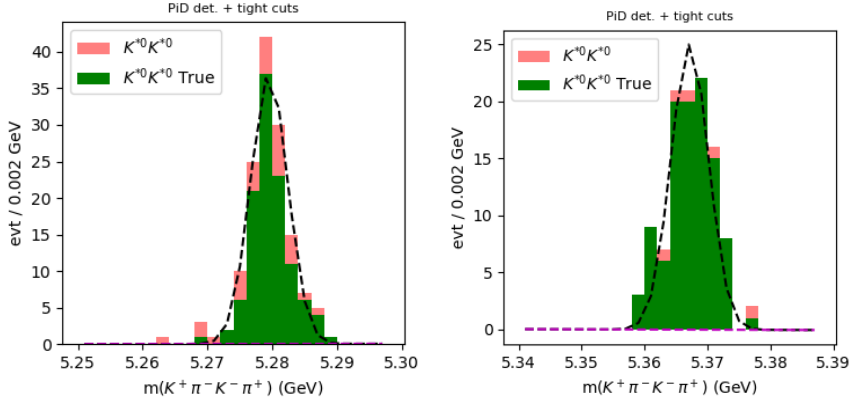


Figure 8: Invariant mass distribution for $\bar{B}_d \rightarrow K^{*0}\bar{K}^{*0}$ and $\bar{B}_s \rightarrow K^{*0}\bar{K}^{*0}$ candidates with particle identification. The data in green are the genuine signal events while the data in red includes non-resonant backgrounds such as $B_{d,s} \rightarrow K^{*0}K^-\pi^+$, $B_{d,s} \rightarrow \bar{K}^{*0}K^+\pi^-$ and at a lower level $B_{d,s} \rightarrow K^\mp\pi^\pm K^\pm\pi^\mp$ as well as the combinatorial background.

where the angle ϕ is the angle between the decay planes of the two vector mesons in the B meson rest frame and $\theta_{1,2}$ are the angles between the direction of motion of $V_{1,2} \rightarrow PP$ pseudoscalar final states and the inverse direction of motion of the B meson as measured in the $V_{1,2}$ rest frame, see Figure 9.

We show in Figure 10 the corresponding distributions for the $\bar{B}^0 \rightarrow K^{*0}\bar{K}^{*0}$ decay. Fitting the angular distributions with the dependences shown in equation (36), one can extract the polarization fractions and estimate the statistical uncertainties. Sensitivities at the level of few ‰ can be reached:

$$\begin{aligned} \sigma_{f_{L,\parallel,\perp}}^{B_d} &\simeq 0.004 \\ \sigma_{f_{L,\parallel,\perp}}^{B_s} &\simeq 0.002 \end{aligned} \quad (37)$$

Such sensitivities would enable one to study in great detail the B decays into two vector states and maybe unravel New Physics.

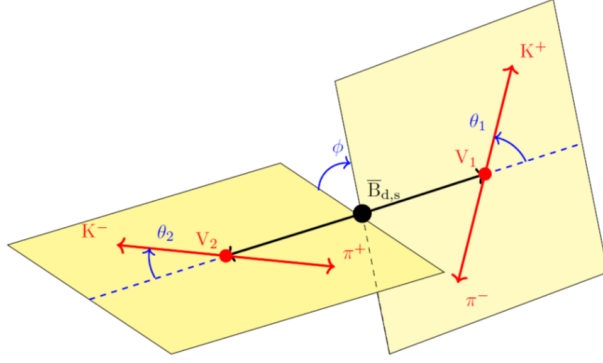


Figure 9: Definition of the angles θ_1 , θ_2 and ϕ for the decay $\bar{B}^0 \rightarrow K^{*0} \bar{K}^{*0}$ used in the angular analysis. Each angle is defined in the rest frame of the decaying particle.

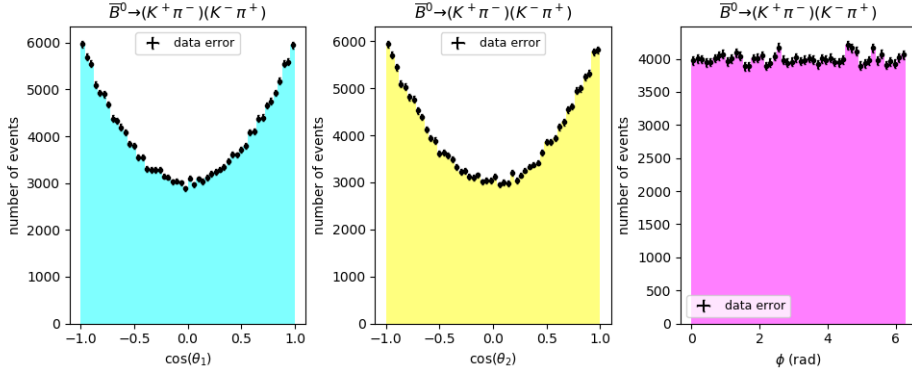


Figure 10: θ_1 , θ_2 and ϕ distributions expected at FCC-ee for the decay $\bar{B}^0 \rightarrow K^{*0} \bar{K}^{*0}$. The expected polarization fractions are $f_L = 0.5$ and $f_{\parallel} = f_{\perp} = 0.25$.

6 Conclusions

In conclusion, we have made evident in a quantitative way that there is a problem of U-spin violation, very much larger than could be expected, in the decays $\bar{B}_{d,s} \rightarrow K^{*0} \bar{K}^{*0}$, a trend that had been suggested by previous authors. This clear feature asks for new measurements, mainly on the decay $\bar{B}_s \rightarrow K^{*0} \bar{K}^{*0}$. For example, should the error on $f_{L, \text{Exp}}$ for $\bar{B}_s \rightarrow K^{*0} \bar{K}^{*0}$ be reduced by a factor 2 in the near future, the significance would exceed 5 standard deviations. On a longer term, FCC-ee would enable to measure the polarizations with outstanding precisions for both $\bar{B}_{d,s}$, allowing one to reveal whether new physics appears in $\bar{B}_{d,s} \rightarrow K^{*0} \bar{K}^{*0}$. More generally, $\bar{B}_{u,d,s} \rightarrow V_1 V_2$ is a very rich area for testing in depth the standard model further.

Acknowledgments

We wish to thank Franco Bedeschi for making his vertexing code available and for very useful discussions about the reconstruction of displaced ver-

tices. We wish to thank also Emmanuel Perez for producing the $Z \rightarrow b\bar{b}$ and $Z \rightarrow c\bar{c}$ simulation samples and for skimming the data. We are also indebted to Joaquim Matias for pointing out to us the interesting references [19, 20].

References

- [1] R. Aleksan and L. Oliver, *Remarks on the penguin decay $B_s \rightarrow \phi\phi$ with prospects for FCC-ee*, arXiv:2205.07823.
- [2] M. Bicer, et al., First look at the physics case of TLEP, J. High Energy Phys. **01** (2014) 164, [https://doi.org/10.1007/JHEP01\(2014\)164](https://doi.org/10.1007/JHEP01(2014)164), arXiv:1308.6176.
- [3] A. Abada, et al., FCC Collaboration, Eur. Phys. J. C **79**(6) (2019) 474, <https://doi.org/10.1140/epjc/s10052-019-6904-3>.
- [4] A. Abada, et al., FCC Collaboration, Eur. Phys. J. ST **228**(2) (2019) 261, <https://doi.org/10.1140/epjst/e2019-900045-4>.
- [5] R.L. Workman, et al., (Particle Data Group), Prog. Theor. Exp. Phys. **2022**, 083C01 (2022) and 2023 update.
- [6] R. Aaij et al. LHCb collaboration, J. High Energy Phys. **07** (2019) 032, arXiv:1905.06662[hep-ex].
- [7] R. Aleksan and L. Oliver, *Analysis of data on B decays into two light vector mesons*, arXiv:2403.19025 [hep-ph].
- [8] J. Charles, A. Le Yaouanc, L. Oliver, O. Pene and J.-C. Raynal, *Heavy-to-Light Form Factors in the Final Hadron Large Energy Limit of QCD*, Phys. Rev. D **60** (1999) 014001, arXiv:hep-ph/9812358; M. Beneke and T. Feldmann, Nucl. Phys. B **592** (2001) 3, hep-ph/0008255.
- [9] M. Beneke, G. Buchalla, M. Neubert and C. Sachrajda, *QCD factorization in $B \rightarrow \pi K, \pi\pi$ decays and extraction of Wolfenstein parameters*, Nucl. Phys. B **606** (2001) 245, arXiv:hep-ph/0104110.
- [10] M. Beneke, G. Buchalla, M. Neubert and C.T. Sachrajda, *QCD factorization for $B \rightarrow \pi\pi$ decays: Strong phases and CP violation in the heavy quark limit*, Phys. Rev. Lett. **83** (1999) 1914, arXiv:hep-ph/9905312.
- [11] M. Beneke, G. Buchalla, M. Neubert and C.T. Sachrajda, *QCD factorization for exclusive, nonleptonic B meson decays: General arguments and the case of heavy light final states*, Nucl. Phys. B **591** (2000) 313, arXiv:hep-ph/0006124.
- [12] M. Beneke, J. Rohrer and D. Yang, *Branching fractions, polarisation and asymmetries of $B \rightarrow VV$ decays*, Nucl. Phys. B **774** (2007) 64, arXiv:0612290[hep-ph].
- [13] A. Kagan, *Polarization in $B \rightarrow VV$ decays*, Phys. Lett. B **601** (2004) 151, arXiv:hep-ph/0405134.
- [14] H.-Y. Cheng and K.-C. Yang, *Branching ratios and polarization in $B \rightarrow VV, VA, AA$ decays*, Phys. Rev. D **78** (2008) 094001, Phys. Rev. D **79** (2009) 039903 (erratum), arXiv:0805.0329.
- [15] M. Bartsch, G. Buchalla and C. Kraus, *$B \rightarrow V_L V_L$ Decays at NLO in QCD*, arXiv:0810.0249.

- [16] M. Ciuchini, M. Pierini and L. Silvestrini, $B_s \rightarrow K^{*0}\bar{K}^{*0}$ decays: the golden channel for new physics searches, Phys. Rev. Lett. **100** (2008) 031802, arXiv:hep-ph/0703137.
- [17] S. Descotes-Genon, J. Matias and J. Virto, Penguin-mediated $B_{d,s} \rightarrow VV$ decays and the $B_s - \bar{B}_s$ mixing angle, Phys. Rev. D **76** 074005 (2007); Erratum-ibid. D **84** (2011) 039901, arXiv:0705.0477.
- [18] S. Descotes-Genon, J. Matias and J. Virto, An analysis of $B_{d,s}$ mixing angles in presence of New Physics and an update of $B_s \rightarrow K^{*0}\bar{K}^{*0}$, Phys. Rev. D **85** (2012) 034010, arXiv:1111.4882.
- [19] M. Algueró, A. Crivellin, S. Descotes-Genon, J. Matias and M. Novoa-Brunet, A new B -flavor anomaly in $B_{d,s} \rightarrow K^{*0}\bar{K}^{*0}$: anatomy and interpretation, JHEP **04** (2021) 066, arXiv:2011.07867 [hep-ph].
- [20] A. Biswas, S. Descotes-Genon, J. Matias and G. Tetlalmatzi-Xolocotzi, A new puzzle in non-leptonic B decays, JHEP **06** (2023) 108, arXiv:2301.10542 [hep-ph].
- [21] P. Ball and R. Zwicky, $B_{d,s} \rightarrow \rho, \omega, K^*, \phi$ Decay Form Factors from Light-Cone Sum Rules Revisited, Phys. Rev. D **71** (2005) 014029, hep-ph/0412079.
- [22] R. Aleksan, L. Oliver and E. Perez, CP violation and determination of the bs "flat" unitarity triangle at FCCee, Phys. Rev. D **105** (2022) 053008, arXiv:2107.02002[hep-ph] (2021).
- [23] C. Bierlich et al., A comprehensive guide to the physics and usage of PYTHIA 8.3, SciPost Phys. Codeb. 2022 (2022) 8, arXiv:2203.11601[hep-ph].
- [24] J. de Favereau, C. Delaere, P. Demin, A. Giammanco, V. Lemaitre, A. Mertens and M. Selvaggi, Delphes 3: a modular framework for fast simulation of a generic collider experiment, JHEP 2014 (Feb, 2014), arXiv:1307.6346 [hep-ex].
- [25] C. Hensens and the FCC software group, <https://github.com/HEP-FCC/FCCAnalyses>.
- [26] F. Bedeschi. Code available as part of the TrackCovariance module of the Delphes package, <https://github.com/delphes/delphes>.
- [27] F. Bedeschi. Presentation at the FCC Physics Performance meeting, October 2023, <https://indico.cern.ch/event/1337943/>.
- [28] J. G. Körner and G. R. Goldstein, Exclusive Nonleptonic Decays of Bottom and Charm Baryons, Phys. Lett. B **89** (1979) 105.